

Amplified Detection of Iron Ion Based on Plasmon Enhanced Fluorescence and Subsequently Fluorescence Quenching

Lin Zhou · Han Zhang · Yanping Luan · Si Cheng · Li-Juan Fan

Received: 17 March 2014 / Revised: 9 April 2014 / Accepted: 10 April 2014 / Published online: 17 September 2014
© The Author(s) 2014. This article is published with open access at Springerlink.com

Abstract A facile and rapid approach for detecting low concentration of iron ion (Fe^{3+}) with improved sensitivity was developed on the basis of plasmon enhanced fluorescence and subsequently amplified fluorescence quenching. $\text{Au}_1\text{Ag}_4@ \text{SiO}_2$ nanoparticles were synthesized and dispersed into fluorescein isothiocyanate (FITC) solution. The fluorescence of the FITC solution was improved due to plasmon enhanced fluorescence. However, efficient fluorescence quenching of the FITC/ $\text{Au}_1\text{Ag}_4@ \text{SiO}_2$ solution was subsequently achieved when Fe^{3+} , with a concentration ranging from 17 nM to 3.4 μM , was added into the FITC/ $\text{Au}_1\text{Ag}_4@ \text{SiO}_2$ solution, whereas almost no fluorescence quenching was observed for pure FITC solution under the same condition. FITC/ $\text{Au}_1\text{Ag}_4@ \text{SiO}_2$ solution shows a better sensitivity for detecting low concentration of Fe^{3+} compared to pure FITC solution. The quantized limit of detection toward Fe^{3+} was improved from 4.6 μM for pure FITC solution to 20 nM for FITC/ $\text{Au}_1\text{Ag}_4@ \text{SiO}_2$ solution.

Keywords Gold–silver alloy · Plasmon enhanced fluorescence · Fluorescence quenching · Iron ion

1 Introduction

Noble metal nanoparticles (NPs), such as Au and Ag, are known to dramatically change the optical properties of nearby fluorophores due to the localized surface plasmon resonance (LSPR) at the surface of the metal NPs [1]. When fluorescent molecules are localized adjacent to metal surface, their fluorescence emission intensity can be altered enormously, forming the basis of plasmon enhanced fluorescence (PEF) [2]. However, if fluorescent molecules are directly in contact with the metal surface, fluorescence quenching would be suffered due to the non-radiative energy and/or charge transfer from molecules to the metal. A nanometer-thin spacer layer, made of either polyelectrolytes or silica, is usually employed to separate the

molecules away from the metal surface to avoid fluorescence quenching [2–4]. The fluorescence of fluorophores can make a continuous transition from fluorescence quenching to fluorescence enhancement with increasing thickness of the silica layer [5–9]. Great attentions have been paid to prepare metal core-silica/fluorophore-shell nanostructure for various applications, such as optical property [7], cellular imaging [10], and photothermal therapy [11]. The excited surface plasmon can deliver significant control over the optical field and enhance the light absorption or fluorescence emission of molecule, which is critical to improving the sensitivity of fluorescence spectroscopy [12].

During the past couple of decades, fluorescence detection offers a promising approach for simple and rapid tracking of heavy metal ions [13, 14]. Contamination of water by metal ions (*e.g.*, mercury, copper, iron) can cause serious environmental and health problems because of acute and/or chronic toxicity to biological organisms [15–17]. Therefore, monitoring of metal ion levels in water is very important for the environment or our health. The conventional detection concentration of metal ion based on

L. Zhou · H. Zhang · Y. Luan · S. Cheng (✉) · L.-J. Fan
Jiangsu Key Laboratory of Advanced Functional Polymer Design and Application, College of Chemistry, Chemical Engineering and Materials Science, Soochow University, 199 Ren-Ai Road, Suzhou 215123, Jiangsu, People's Republic of China
e-mail: chengsi@suda.edu.cn

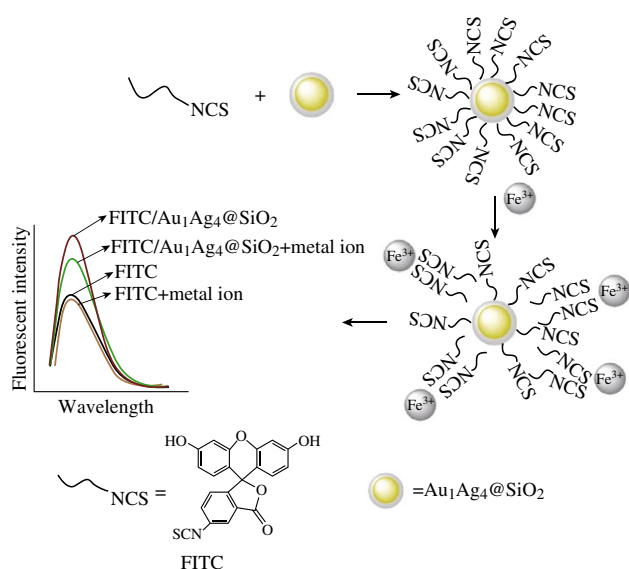


Fig. 1 Schematic illustration of the detection of Fe³⁺ on the basis of fluorescence enhancement and subsequently fluorescence quenching

fluorophore or conjugated polymer is on the micromolar (μM) level [12, 18]. Therefore, many AuNPs-based colorimetric, fluorescent or refractive index sensor have been developed to detect lower concentration of metal ions through utilizing fluorescent noble metal nanoclusters or metal NPs fluorescently labeled DNA nanohybrids structures [9, 15–17, 19–23]. However, complicated processes together with expensive fluorophores or coupling reagents for labeling the probes and/or target analytes were involved in the preparation of fluorophore conjugated AuNPs probes [24]. Specialized synthetic skills and complicated purification procedures are rather time-consuming and disadvantage for further practical application. Thus, developing a facile, rapid, and label-free strategy for the detection of metal ions is still highly desired.

Fluorescein isothiocyanate (FITC) has many reactive groups, such as isothiocyanate group ($-\text{N}=\text{C}=\text{S}$), carboxylic group, hydroxyl group, and carbonyl group (Fig. 1). It has been widely used as a fluorescent label to attach to proteins via the amine group or been tailored for various chemical and biological applications due to different attachment groups, high fluorescence intensity, and great photostability [24–26]. FITC molecules can be readily attached to the surface of AuNPs through their isothiocyanate group [25, 27] and the isothiocyanate group of FITC can also be bond with iron ion (Fe^{3+}) to form metal-isothiocyanate complexes [28].

Herein, we developed a facile and rapid approach to detecting low concentration of Fe^{3+} with improved sensitivity on the basis of plasmon enhanced fluorescence and subsequently amplified fluorescence quenching. First, the fluorescence of the FITC solution was greatly improved by

the addition of Au₁Ag₄@SiO₂ NPs. And then, the fluorescence of solution was dramatically quenched again when Fe^{3+} was added. The extent of fluorescence quenching for the FITC/Au₁Ag₄@SiO₂ solution toward Fe^{3+} is apparently larger than that for pure FITC solution, which resulted in the improved sensitivity for detecting low concentration of Fe^{3+} .

2 Experimental Methods

Au₁Ag₄ alloy NPs were synthesized by reducing HAuCl₄ and AgNO₃ solution simultaneously with sodium citrate, according to a reported procedure with slight modifications [30]. 6 mL of HAuCl₄ aqueous solution (0.01 mol/L) and 24 mL of AgNO₃ aqueous solution (0.01 mol/L) were added to 70 mL ultra-filtered water. The mixture was heated to boiling, and then 6 mL of sodium citrate aqueous solution (1 wt%) was injected quickly. The mixture was further boiled for about 60 min and the color of the solution turned from colorless to yellow within 10 min. Subsequently, 6 mL of sodium citrate aqueous solution was injected again. The mixture was kept boiling for 60 min and then cooled to room temperature.

100 mL of as-synthesized Au₁Ag₄ alloy NPs was centrifuged at 6,500 rpm, and then was redispersed into 3 mL of water. 1 mL of concentrated Au₁Ag₄ alloy NPs were added into 30 mL of iso-propanol/9 mL of deionized water mixture with vigorous stirring. Different volume of TEOS (10 mM in iso-propanol) was added to the reaction mixture immediately followed by the addition of 0.75 mL of 25 % ammonium hydroxide. The Au₁Ag₄@SiO₂ NPs with different silica thicknesses were made by tuning the volume of TEOS to 1.6, 3.2, 4.8, and 6.0 mL. The reaction solution was kept at 30 °C for 24 h under stirring.

In a typical process, 400 μL Au₁Ag₄@SiO₂ solution was added to 2.5 mL FITC aqueous solution (5×10^{-6} M), then different volumes of Fe^{3+} solutions were added. In order to eliminate the possibility of contaminations, Fe^{3+} solutions were prepared by dissolving desired amount of solid FeCl_3 (AR) into ultra-filtered water. The mixture was obtained by repeated gentle inversion for 10 s and then was directly measured for fluorescence emission spectra. Ultra-filtered water was used in all experiments.

Transmission electron microscope (TEM) was taken with TecnaiG220, FEI company microscope operated at 200 kV. Ultraviolet–visible spectroscopy (UV-Vis) extinction spectra were measured with Shimadzu UV-3150 spectrophotometer. Fluorescence emission measurements were recorded with a Horiba FluoroMax-4 spectrofluorometer. Fluorescence lifetimes were performed on FL3-TCSPC Fluorescence Spectroscopy (Horiba Jobin–Yvon Inc., France).

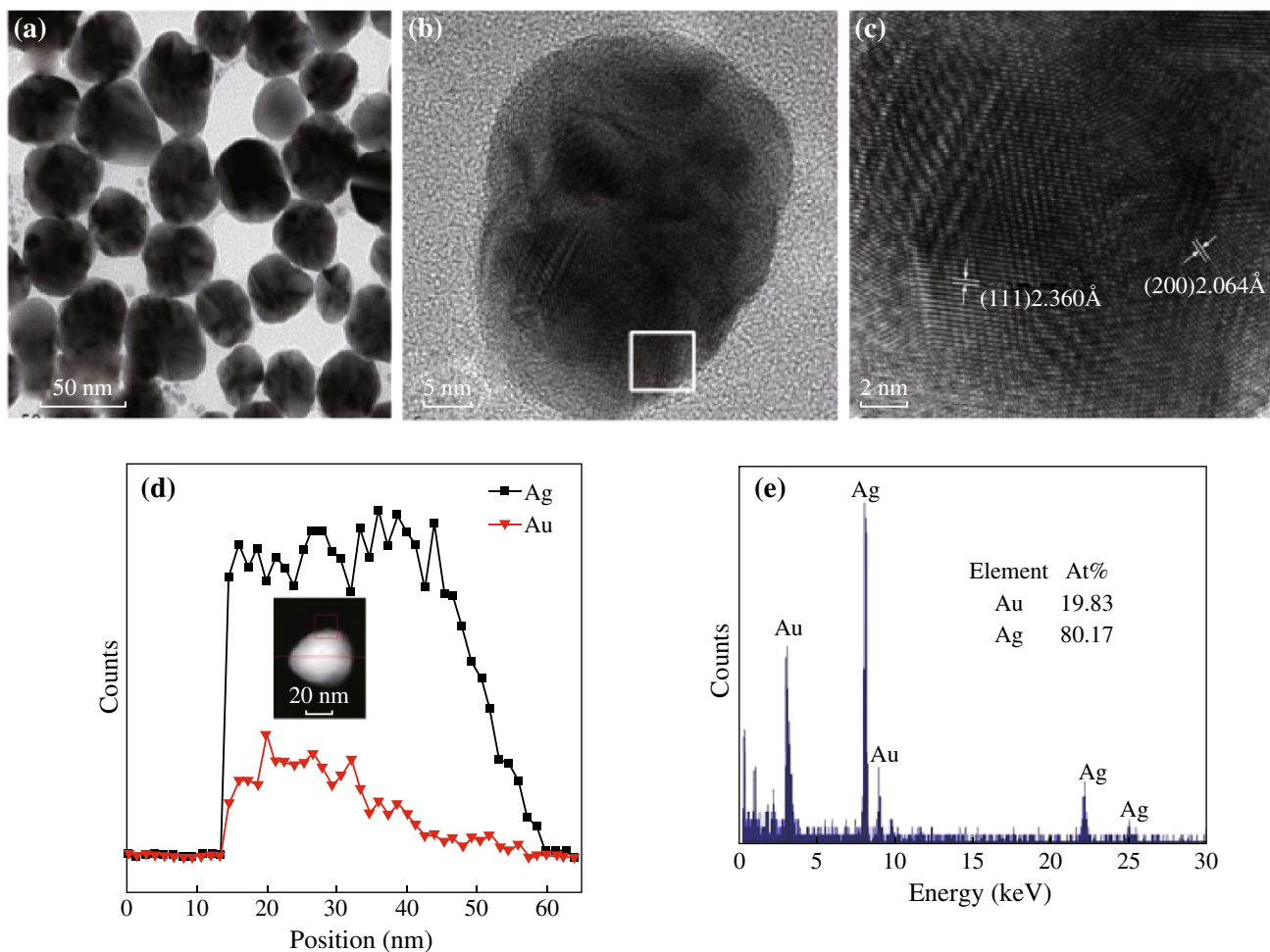


Fig. 2 **a** TEM image of Au₁Ag₄ alloy NPs. **b** and **c** High-resolution electron images of Au₁Ag₄ NPs. **d** Cross-sectional compositional STEM-EDS line scan profiles recorded from one nanoparticle. Inset is HAADF-STEM image. **e** TEM-EDS spectrum of a single Au₁Ag₄ NPs

3 Results and Discussion

Our strategy for fluorescence enhancement was to disperse as-synthesized Au₁Ag₄@SiO₂ NPs into FITC solution. The fluorescence of the FITC solution was improved with the addition of Au₁Ag₄@SiO₂ NPs due to PEF. However, the field enhancement region of metal NPs are confined in close vicinity to the surface of plasmonic metal NPs and the fluorescence enhancement is very sensitive to the surrounding environment of metal NPs [2], such as the space between fluorescent molecule and metal NPs. Thus, the previous enhanced fluorescence of FITC by the Au₁Ag₄@SiO₂ NPs was dramatically quenched again when Fe³⁺ was dropped into the FITC/Au₁Ag₄@SiO₂ solution. The fluorescence quenching is possibly attributed to the complexation action between the isothiocyanate group of FITC and Fe³⁺, which resulted that FITC molecule was away from the field enhancement region of Au₁Ag₄@SiO₂ NPs (Fig. 1).

Note that the local electric field enhancement is dependent on the plasmon resonance wavelength of metal NPs. The fluorescence intensity reaches to the maximum when the plasmon wavelength of the metal NPs is between the absorption and emission peak of the fluorescent molecules [29]. However, localized plasmonic resonances have certain peak widths due to damping; the maximal effect is also believed to occur when the emission or excitation peak overlaps closely with the plasmon resonance peak [2]. Only when a plasmon resonance is excited at its peak wavelength can the maximal field enhancement be obtained [2]. We synthesized Au₁Ag₄ NPs with an extinction peak at 437 nm by the co-reduction of chlorauric acid (HAuCl₄) and silver nitrate (AgNO₃) solution according to a reported procedure with slight modifications [30]. The average diameter of Au₁Ag₄ NPs is 35 ± 5 nm. The High-resolution TEM (HRTEM) images of the Au₁Ag₄ NPs showed the d-spacing for lattice fringes and the corresponding selected area matched well with that of the (111) and (200)

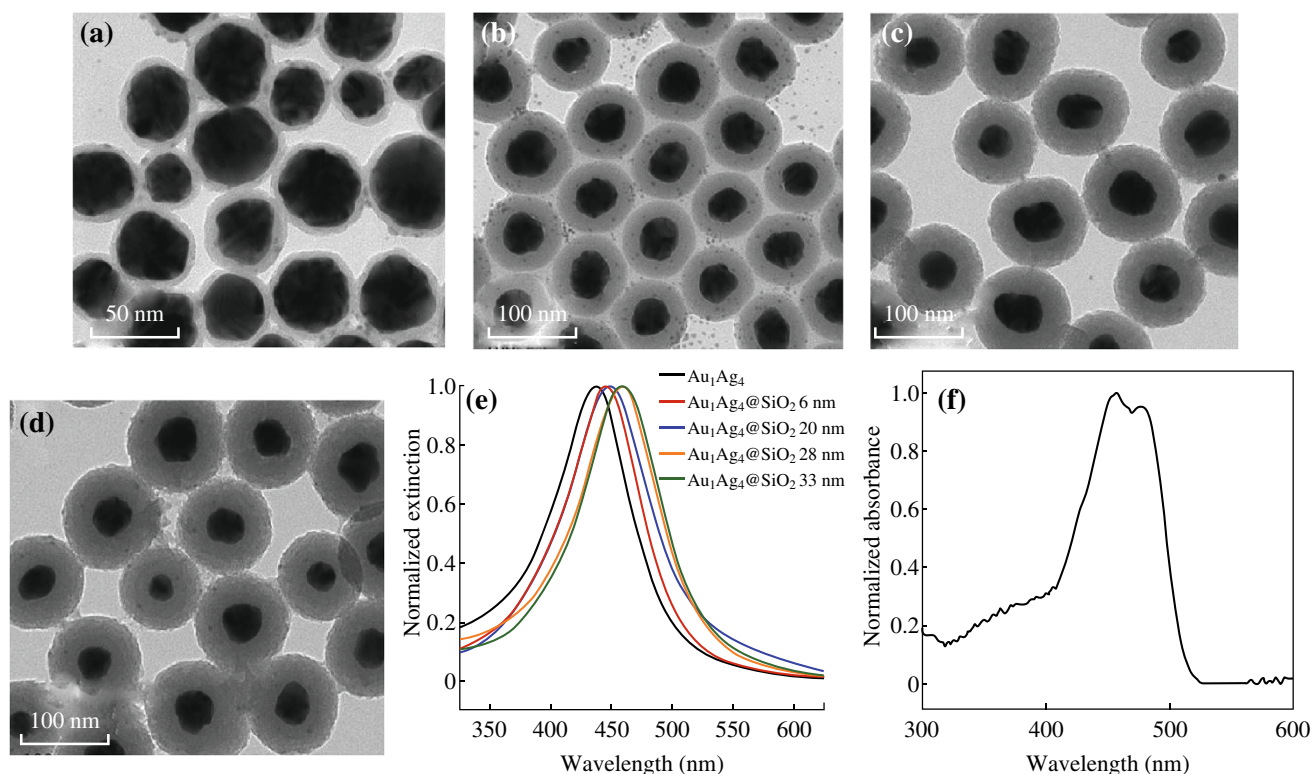


Fig. 3 TEM images of $\text{Au}_1\text{Ag}_4@\text{SiO}_2$ with different thicknesses of silica shells: **a** 6 nm; **b** 20 nm; **c** 28 nm; **d** 33 nm. **e** The corresponding extinction spectra. **f** UV-Vis spectrum of the FITC solution

planes of face-centered cubic Au and Ag (Fig. 2). High-angle annular dark-field (HAADF) scanning transmission electron microscopy (STEM) image with energy dispersive X-ray spectroscopic (EDX) elemental line profiling and TEM-EDS (TEM-energy dispersive spectrum) of single NPs revealed the alloy structure and composition of NPs (Fig. 2).

A SiO_2 shell with variable thicknesses was coated on the surface of Au_1Ag_4 NPs by a sol-gel reaction of TEOS according to the reported process [24]. The fluorescent molecule-metal distance was controlled by varying the thickness of the SiO_2 spacer shell. The surface plasmon resonance peak of $\text{Au}_1\text{Ag}_4@\text{SiO}_2$ NPs red-shifted from 445 to 458 nm as the thickness of the silica shell increased from 6 nm to 33 nm (Fig. 3a–e). The extinction peak of $\text{Au}_1\text{Ag}_4@\text{SiO}_2$ NPs is close to the absorption peak of the FITC solution (454–474 nm) (Fig. 3f). The silica layer not only provided a distance-dependent PEF but also offered the robustness, chemical inertness, and the versatility needed for the conjugation of fluorescent molecule [4, 7, 31].

Subsequently, $\text{Au}_1\text{Ag}_4@\text{SiO}_2$ NPs were directly dispersed into the FITC solution and the influence of $\text{Au}_1\text{Ag}_4@\text{SiO}_2$ NPs on the fluorescence of the FITC (1×10^{-5} M) were investigated. The emission spectra of the FITC/ $\text{Au}_1\text{Ag}_4@\text{SiO}_2$ solution as well as pure FITC

solution are presented in Fig. 4a. The fluorescence of the FITC solution increased greatly as the thickness of the silica shell varied. Maximal fluorescence intensity (about 2.7 times) was observed when the thickness of silica shell was 33 nm. Enhanced fluorescence is also easily discernible to the naked eye under 365 nm irradiation (the photos inset in Fig. 4a). The fluorescence enhancement can also be achieved when decreasing the concentration of FITC aqueous solution. The max fluorescence intensity of the FITC/ $\text{Au}_1\text{Ag}_4@\text{SiO}_2$ solution is 1.9, 2.0, and 3.0 folds of pure FITC solution, corresponding to the FITC solution with a concentration of 5×10^{-6} , 1×10^{-7} , and 5×10^{-8} M, respectively (Fig. 4b–d).

In general, the field-enhanced fluorescence is very sensitive to the surrounding environment of metal NPs. Note that the fluorescence of the solution was varied as the thickness of silica shell changed, we further investigated the metal ion-responsive property of the FITC/ $\text{Au}_1\text{Ag}_4@\text{SiO}_2$ solution. The fluorescence response of the FITC and FITC/ $\text{Au}_1\text{Ag}_4@\text{SiO}_2$ solution toward Fe^{3+} with a concentration ranging from 17 nM to 63 μM were compared and their fluorescence spectra were recorded (Fig. 5). We found that 34 nM Fe^{3+} was enough to show efficient fluorescent quenching (14 %) of the FITC/ $\text{Au}_1\text{Ag}_4@\text{SiO}_2$ solution, whereas no fluorescence quenching was observed in pure

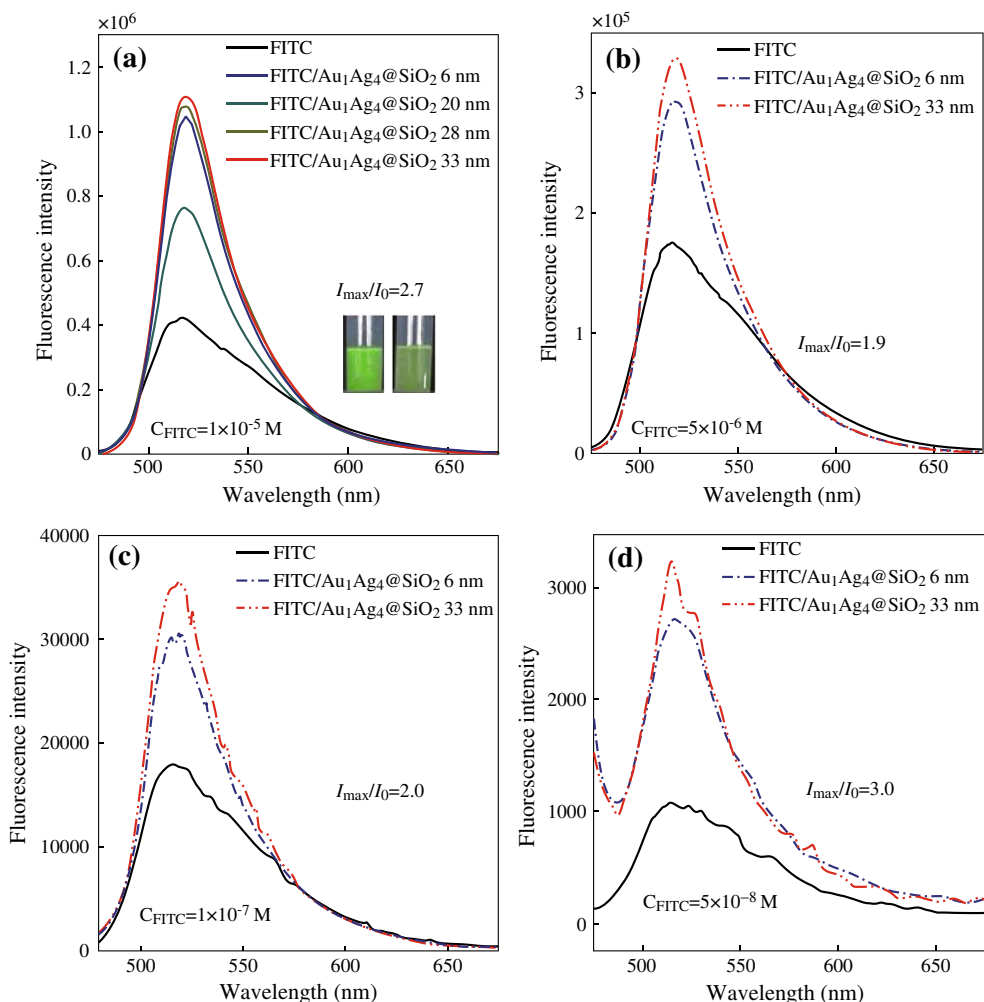


Fig. 4 Fluorescence emission spectra of the FITC solution with the addition of Au₁Ag₄@SiO₂ NPs. The concentration of the FITC solution is: **a** 1×10^{-5} M; **b** 5×10^{-6} M; **c** 1×10^{-7} M and **d** 5×10^{-8} M, respectively. The volume of the FITC solution is 2.5 mL. The excitation wavelength is 450 nm

FITC solution. An apparent fluorescence quenching of pure FITC solution was found until Fe³⁺ concentration reached 3.4 μM. The fluorescence intensity of the solution kept decreasing as the concentration of Fe³⁺ increased. About 32 and 68 % of quenching toward 3.4 and 32 μM of Fe³⁺ were achieved for FITC/Au₁Ag₄@SiO₂ solution, but only about 11 and 43 % of quenching were observed in pure FITC solution under the same condition (Fig. 6). Relative fluorescence intensity ($(I_0 - I)/I_0$) of the FITC solution and FITC/Au₁Ag₄@SiO₂ solution toward Fe³⁺ with a concentration ranging from 17 nM to 63 μM was shown in Fig. 6. The relative fluorescence intensity displayed in Fig. 6, indicated that the extent of fluorescence quenching of the FITC/Au₁Ag₄@SiO₂ solution upon Fe³⁺ was apparently larger than that in FITC solution and the sensitivity of detecting low concentration of Fe³⁺ was dramatically improved.

The intensity ratio I_0/I of pure FITC solution and FITC/Au₁Ag₄@SiO₂ solution displayed a good linear relationship versus Fe³⁺ concentration ranging from 3.4 to 63 μM, which was easily described by the Stern–Volmer equation ($I_0/I = 1 + K_{sv}[Q]$), where I_0 and I are the fluorescence intensity of the FITC solution in the absence and presence of metal ion, K_{sv} is the Stern–Volmer fluorescence quenching constant, and Q is the concentration of metal ion. The resulting linear equations were $I_0/I = 1 + 0.027[Fe^{3+}]$ and $I_0/I = 1 + 0.074[Fe^{3+}]$, corresponding to FITC solution and FITC/Au₁Ag₄@SiO₂ solution, respectively. However, the intensity ratio I_0/I for FITC/Au₁Ag₄@SiO₂ solution displayed a different response versus lower concentration of Fe³⁺ ranging from 17 nM to 3.4 μM. A quantitative analysis of Fe³⁺ at the lower concentration was achievable ($I_0/I = 1 + 2.84[Fe^{3+}]$, $R^2 = 0.9498$). The quantized limit of

Fig. 5 Fluorescence spectra of **a** FITC and **c** FITC/ $\text{Au}_1\text{Ag}_4@ \text{SiO}_2$ in the presence of Fe^{3+} . **b** and **d** The corresponding relationship between intensity ratio (I_0/I) and Fe^{3+} concentration. The excitation wavelength is 450 nm

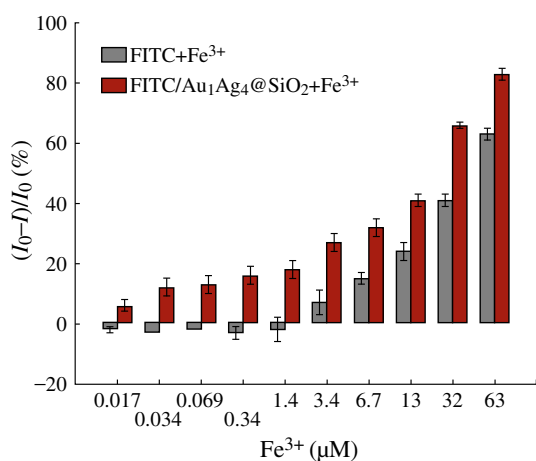
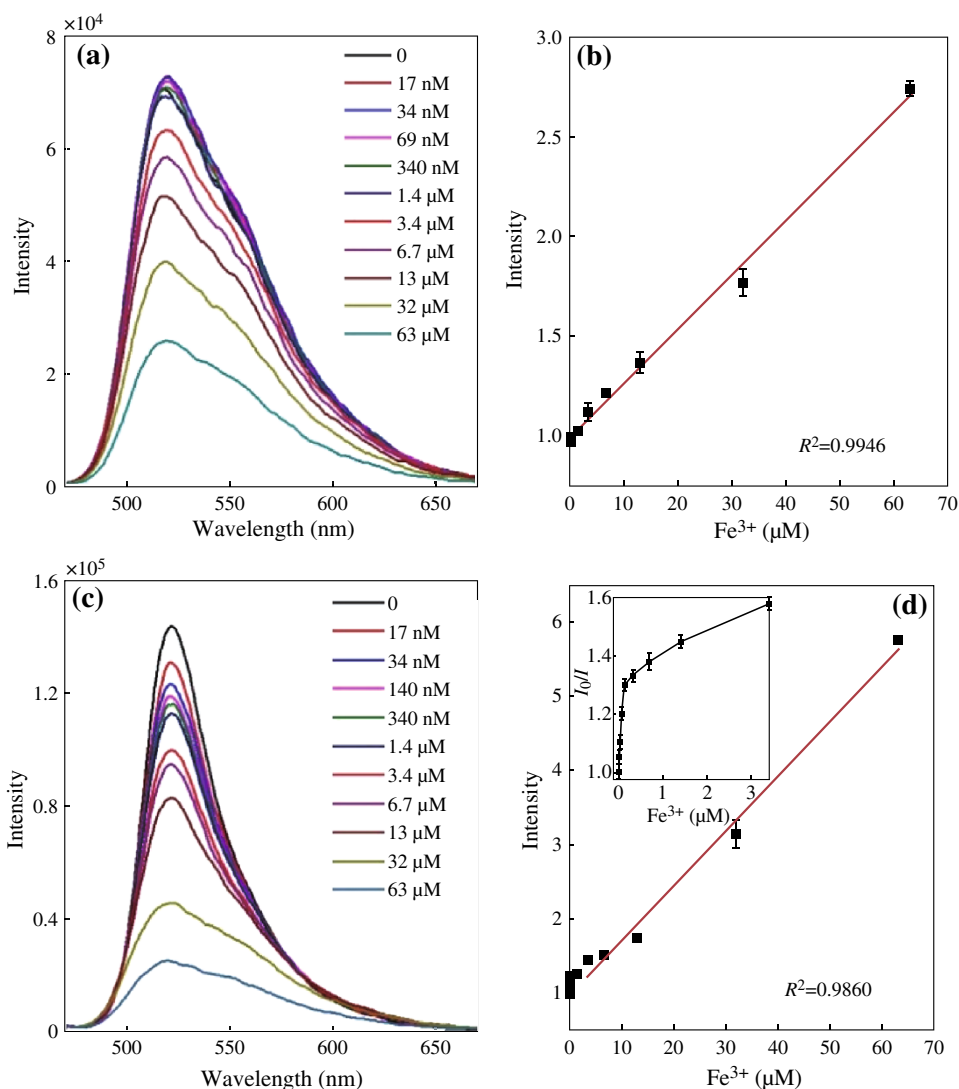
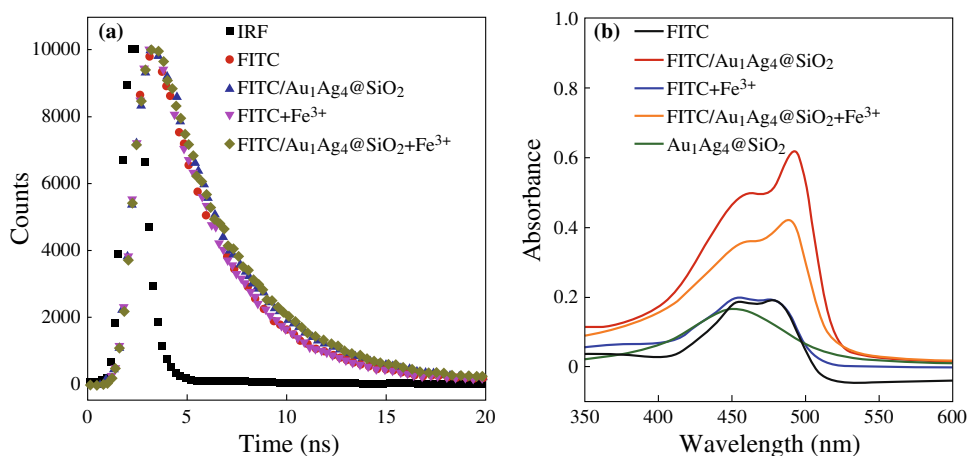


Fig. 6 Relative fluorescence intensity ($(I_0 - I)/I_0$) of the FITC solution and FITC/ $\text{Au}_1\text{Ag}_4@ \text{SiO}_2$ solution toward Fe^{3+} with a concentration from 17 nM to 63 μM

detection (LOD) toward Fe^{3+} was calculated to be 20 nM, whereas the LOD value for pure FITC solution toward Fe^{3+} is only 4.6 μM .

We preliminarily investigated the possible reasons for fluorescence enhancement and subsequently fluorescence quenching in this system. Usually, the PEF arises from two contributions. One is the increase in the radiative emission rate, which leads to very short fluorescence lifetime. The other is the increase in the excitation rate due to the local electric field enhancement near the surfaces of metal NPs, which result in surface plasmon enhanced absorption [1, 32, 33]. Figure 7a shows the time-resolved measurements on the emission dynamics of the FITC solution without and in the presence of $\text{Au}_1\text{Ag}_4@ \text{SiO}_2$ NPs. No notable decrease of the fluorescence lifetimes were observed for pure FITC solution and FITC/ $\text{Au}_1\text{Ag}_4@ \text{SiO}_2$ solution. The addition of Fe^{3+} also has no influence on the fluorescent lifetimes.

Fig. 7 **a** The fluorescence intensity decays of FITC and FITC/Au₁Ag₄@SiO₂ solution without or with Fe³⁺. The instrument response function (IRF) is also included. The concentration of Fe³⁺ is 3.4 μM. **b** Absorption spectra of the FITC solution, Au₁Ag₄ NPs and the FITC solution in the absence or presence of Au₁Ag₄@SiO₂ NPs or Fe³⁺. The concentration of Fe³⁺ is 340 nM



However, the absorption peak of FITC was greatly improved when Au₁Ag₄@SiO₂ NPs were added (Fig. 7b). It is because that plasmonic metal NPs exhibit large absorption and scattering cross sections. So the fluorescence emission from one fluorescence molecule-nanoparticles hybrid nanostructures can be absorbed or scattered by the other hybrid NPs in the solution if the fluorescence emission peak overlaps with the plasmon resonance peak [2]. The fluorescence lifetime data and absorption spectra suggested that the electric field enhanced absorption is the dominant factor in our system. Moreover, the absorption of the FITC/Au₁Ag₄@SiO₂ solution dramatically decreased after the addition of Fe³⁺ (Fig. 7b), indicating that the aggregation status of FITC molecules changed after the addition of Fe³⁺. The reason may be attributed to the complexation between isothiocyanate group and Fe³⁺. Isothiocyanate group of FITC can interact with the Fe³⁺ to form metal-isothiocyanate complexes [28]. When the Fe³⁺ was dropped into the FITC solution, bridges would be formed between FITC molecules and possibly induced FITC molecules to aggregate. The aggregation of FITC results in the FITC molecule being dropped away from the silica layer as well as the field enhancement region of NPs and the previously enhanced fluorescence of FITC by Au₁Ag₄@SiO₂ NPs were greatly quenched again due to the promoted distance between FITC molecule and metal NPs.

4 Conclusions

A facile and rapid approach for detecting low concentration of Fe³⁺ with improved sensitivity was developed through plasmon enhanced fluorescence and subsequently amplified fluorescent quenching. The fluorescence of the FITC solution was greatly improved by Au₁Ag₄@SiO₂ due to the plasmon enhanced fluorescence. The enhanced fluorescence arises from surface plasmon enhanced absorption. However,

efficient fluorescent quenching of the FITC solution was obtained when Fe³⁺ with a concentration ranging from 17 nM to 3.4 μM was further added into the FITC/Au₁Ag₄@SiO₂ mixture, whereas no fluorescence quenching was observed for pure FITC solution. The amplified fluorescence quenching results in a great increase of sensitivity for detecting low concentration of metal ion. The quantized limit of detection (LOD) was improved from 4.6 μM for pure FITC solution to 20 nM for FITC/Au₁Ag₄@SiO₂ solution. We believe this work would provide a general approach for preparing plasmonic chemsensor with high sensitivity for the detection of low concentration of metal ions.

Acknowledgments This work is supported by the National Natural Science Foundation of China (51003069), Natural Science Foundation of Jiangsu Higher Education Institutions of China (10KJB430014) and A Project Funded by the Priority Academic Program Development of Jiangsu Higher Education Institutions.

Open Access This article is distributed under the terms of the Creative Commons Attribution License which permits any use, distribution, and reproduction in any medium, provided the original author(s) and the source are credited.

References

1. W.H. Ni, Z. Yang, H.J. Chen, L. Li, J.F. Wang, Coupling between molecular and plasmonic resonances in freestanding dye-gold nanorod hybrid nanostructures. *J. Am. Chem. Soc.* **130**(21), 6692–6693 (2008). doi:10.1021/ja8012374
2. T. Ming, H.J. Chen, R.B. Jiang, Q. Li, J.F. Wang, Plasmon-controlled fluorescence: beyond the intensity enhancement. *J. Phys. Chem. Lett.* **3**(2), 191–202 (2012). doi:10.1021/jz201392k
3. G. Schneider, G. Decher, Distance-dependent fluorescence quenching on gold nanoparticles ensheathed with layer-by-layer assembled polyelectrolytes. *Nano Lett.* **6**(3), 530–536 (2006). doi:10.1021/nl052441s
4. P. Reineck, D. Gómez, S.H. Ng, M. Karg, T. Bell, P. Mulvaney, U. Bach, Distance and wavelength dependent quenching of molecular fluorescence by Au@SiO₂ core-shell nanoparticles. *ACS Nano* **7**(8), 6636–6648 (2013). doi:10.1021/nm401775e

5. A.R. Guerrero, R.F. Aroca, Surface-enhanced fluorescence with shell-isolated nanoparticles (SHINEF). *Angew. Chem. Int. Ed.* **50**(3), 665–668 (2011). doi:[10.1002/anie.201004806](https://doi.org/10.1002/anie.201004806)
6. D.M. Cheng, Q.H. Xu, Separation distance dependent fluorescence enhancement of fluorescein isothiocyanate by silver nanoparticles. *Chem. Commun.* **3**, 248–250 (2007). doi:[10.1039/B612401A](https://doi.org/10.1039/B612401A)
7. K. Aslan, M. Wu, J.R. Lakowicz, C.D. Geddes, Fluorescent core-shell Ag@SiO₂ nanocomposites for metal-enhanced fluorescence and single nanoparticle sensing platforms. *J. Am. Chem. Soc.* **129**(6), 1524–1525 (2007). doi:[10.1021/ja0680820](https://doi.org/10.1021/ja0680820)
8. J.P. Yang, F. Zhang, Y.R. Chen, S. Qian, P. Hu, W. Li, Y.H. Deng, Y. Fang, L. Han, M. Luqman, D.Y. Zhao, Core-shell Ag@SiO₂@mSiO₂ mesoporous nanocarriers for metal-enhanced fluorescence. *Chem. Commun.* **47**(42), 11618–11620 (2011). doi:[10.1039/C1CC15304H](https://doi.org/10.1039/C1CC15304H)
9. C. Wu, J. Zheng, C. Huang, J. Lai, S. Li, C. Chen, Y. Zhao, Hybrid silica-nanocrystal-organic dye superstructures as post-encoding fluorescent probes. *Angew. Chem. Int. Ed.* **46**(28), 5393–5396 (2007). doi:[10.1002/anie.200700847](https://doi.org/10.1002/anie.200700847)
10. V.W.K. Ng, R. Berti, F. Lesage, A. Kakkar, Gold: a versatile tool for in vivo imaging. *J. Mater. Chem. B* **1**(1), 9–25 (2013). doi:[10.1039/C2TB00020B](https://doi.org/10.1039/C2TB00020B)
11. Z.J. Zhang, J. Wang, C.Y. Chen, Gold nanorods based platforms for light-mediated theranostics. *Theranostics* **3**(3), 223–238 (2012). doi:[10.7150/thno.5409](https://doi.org/10.7150/thno.5409)
12. H.M. Su, Y.C. Zhong, T. Ming, J.F. Wang, K.S. Wong, Extraordinary surface plasmon coupled emission using core/shell gold nanorods. *J. Phys. Chem. C* **116**(16), 9259–9264 (2012). doi:[10.1021/jp211713y](https://doi.org/10.1021/jp211713y)
13. J. Song, W. Zhang, K.S. Miao, H.L. Zeng, S. Cheng, L.J. Fan, Receptor-free poly (phenylenevinylene) fibrous membranes for cation sensing: high sensitivity and good selectivity achieved by choosing the appropriate polymer matrix. *Appl. Mater. Interfaces* **5**(10), 4011–4016 (2013). doi:[10.1021/am4005336](https://doi.org/10.1021/am4005336)
14. D.Z. Shen, L.S. Wang, Z.X. Pan, S. Cheng, X.L. Zhu, L.J. Fan, Toward a highly sensitive fluorescence sensing system of an amphiphilic molecular rod: facile synthesis and significant solvent-assisted photophysical tunability. *Macromolecules* **44**(4), 1009–1015 (2011). doi:[10.1021/ma102311n](https://doi.org/10.1021/ma102311n)
15. G. Sener, L. Uzun, A. Denizli, Lysine promoted colorimetric response of gold nanoparticles: a simple assay for ultra-sensitive mercury (II) detection. *Anal. Chem.* **86**(1), 514–520 (2014). doi:[10.1021/ac403447a](https://doi.org/10.1021/ac403447a)
16. T.Y. Zhou, L.P. Lin, M.C. Rong, Y.Q. Jiang, X. Chen, Silver-gold alloy nanoclusters as a fluorescence-enhanced probe for aluminum ion sensing. *Anal. Chem.* **85**(20), 9839–9844 (2013). doi:[10.1021/ac4023764](https://doi.org/10.1021/ac4023764)
17. Z.Q. Yuan, N. Cai, Y. Du, Y. He, E.S. Yeung, Sensitive and selective detection of copper ions with highly stable polyethyleneimine-protected silver nanoclusters. *Anal. Chem.* **86**(1), 419–426 (2014). doi:[10.1021/ac402158j](https://doi.org/10.1021/ac402158j)
18. X.F. Wu, B.W. Xu, H. Tong, L.X. Wang, Phosphonate-functionalized polyfluorene film sensors for sensitive detection of iron (III) in both organic and aqueous media. *Macromolecules* **43**(21), 8917–8923 (2010). doi:[10.1021/ma1019413](https://doi.org/10.1021/ma1019413)
19. X. He, H. Liu, Y. Li, S. Wang, Y. Li, N. Wang, J. Xiao, X. Xu, D. Zhu, Gold nanoparticle-based fluorometric and colorimetric sensing of copper (II) ions. *Adv. Mater.* **17**(23), 2811–2815 (2005). doi:[10.1002/adma.200501173](https://doi.org/10.1002/adma.200501173)
20. J.P. Xie, Y.G. Zheng, J.Y. Ying, Highly selective and ultrasensitive detection of Hg²⁺ based on fluorescence quenching of Au nanoclusters by Hg²⁺-Au⁺ interactions. *Chem. Commun.* **46**(6), 961–963 (2010). doi:[10.1039/B920748A](https://doi.org/10.1039/B920748A)
21. Y.S. Wu, F.F. Huang, Y.W. Lin, Fluorescent detection of lead in environmental water and urine samples using enzyme mimics of catechin-synthesized Au nanoparticles. *Appl. Mater. Interfaces* **5**(4), 1503–1509 (2013). doi:[10.1021/am3030454](https://doi.org/10.1021/am3030454)
22. J.W. Liu, Y. Lu, A DNAzyme catalytic beacon sensor for paramagnetic Cu²⁺ ions in aqueous solution with high sensitivity and selectivity. *J. Am. Chem. Soc.* **129**(32), 9838–9839 (2007). doi:[10.1021/ja0717358](https://doi.org/10.1021/ja0717358)
23. D.B. Liu, Z. Wang, X.Y. Jiang, Gold nanoparticles for the colorimetric and fluorescent detection of ions and small organic molecules. *Nanoscale* **3**(4), 1421–1433 (2011). doi:[10.1039/C0NR00887G](https://doi.org/10.1039/C0NR00887G)
24. S.C. Wei, P.H. Hsu, Y.F. Lee, Y.W. Lin, C.C. Huang, Selective detection of iodide and cyanide anions using gold-nanoparticle-based fluorescent probes. *ACS Appl. Mater. Interfaces* **4**(5), 2652–2658 (2012). doi:[10.1021/am3003044](https://doi.org/10.1021/am3003044)
25. C.Y. Lin, C.H. Liu, W.L. Tseng, Fluorescein isothiocyanate-capped gold nanoparticles for fluorescent detection of reactive oxygen species based on thiol oxidation and their application for sensing glucose in serum. *Anal. Methods* **2**(11), 1810–1815 (2010). doi:[10.1039/C0AY00428F](https://doi.org/10.1039/C0AY00428F)
26. J.H. Choi, H.S. Kim, J.W. Choi, J.W. Hong, Y.K. Kim, B.K. Oh, A novel Au-nanoparticle biosensor for the rapid and simple detection of PSA using a sequence-specific peptide cleavage reaction. *Biosens. Bioelectron.* **49**, 415–419 (2013). doi:[10.1016/j.bios.2013.05.042](https://doi.org/10.1016/j.bios.2013.05.042)
27. B. Hu, Y. Zhao, H.Z. Zhu, S.H. Yu, Selective chromogenic detection of thiol-containing biomolecules using carbonaceous nanospheres loaded with silver nanoparticles as carrier. *ACS Nano* **5**(4), 3166–3171 (2011). doi:[10.1021/nn2003053](https://doi.org/10.1021/nn2003053)
28. R. Clark, C.S. Williams, Infra-red spectra (3000–200 cm⁻¹) of metal-isothiocyanate complexes. *Spectrochim. Acta* **22**(6), 1081–1090 (1966). doi:[10.1016/0371-1951\(66\)80198-4](https://doi.org/10.1016/0371-1951(66)80198-4)
29. Y.C. Chen, K. Munechika, D.S. Ginger, Dependence of fluorescence intensity on the spectral overlap between fluorophores and plasmon resonant single silver nanoparticles. *Nano Lett.* **7**(3), 690–696 (2007). doi:[10.1021/nl062795z](https://doi.org/10.1021/nl062795z)
30. S. Link, Z.L. Wang, M.A. El-Sayed, Alloy formation of gold-silver nanoparticles and the dependence of the plasmon absorption on their composition. *J. Phys. Chem. B* **103**(18), 3529–3533 (1999). doi:[10.1021/jp990387w](https://doi.org/10.1021/jp990387w)
31. A.G. Martinez, J.P. Juste, L.M. Liz-Marzan, Recent progress on silica coating of nanoparticles and related nanomaterials. *Adv. Mater.* **22**(11), 1182–1195 (2010). doi:[10.1002/adma.200901263](https://doi.org/10.1002/adma.200901263)
32. H.J. Chen, T. Ming, L. Zhao, F. Wang, L.D. Sun, J.F. Wang, C.H. Yan, Plasmon-molecule interactions. *Nano Today* **5**(5), 494–505 (2010). doi:[10.1016/j.nantod.2010.08.009](https://doi.org/10.1016/j.nantod.2010.08.009)
33. O. Stranik, R. Nooney, C. McDonagh, B.D. MacCraith, Optimization of nanoparticle size for plasmonic enhancement of fluorescence. *Plasmonics* **2**(1), 15–22 (2007). doi:[10.1007/s11468-006-9020-9](https://doi.org/10.1007/s11468-006-9020-9)